

## Measurements of Motions and Magnetic Characteristics of Red Blood Cells in Microchannel Flows in the Presence of Magnetic Field

K. Tatsumi<sup>1,2,\*</sup>, Y. Komori<sup>1</sup>, K. Nakabe<sup>1,2</sup>

<sup>1</sup>Department of Mechanical Engineering and Science, Kyoto University, Kyoto, Japan

<sup>2</sup>Advanced Research Institute of Fluid Science and Engineering, Kyoto University, Japan

\*Corresponding author, E-mail: tatsumi@me.kyoto-u.ac.jp

### ABSTRACT

In the present study, measurement of the bulk susceptibility of the RBC is described. Measurements were carried out by visualizing the RBC motions in the presence of the magnetic field gradient using the microchannel and high-speed camera. The RBC suspended fluid was supplied to the microchannel, which was placed in the bore of the magnetic field generator. A uniform magnetic field of which the intensities were 4 and 8T were generated in the bore. Measurements of the bulk susceptibility of the RBC were carried out using a microchannel, the bottom wall of which was made of nickel (ferromagnetic body). This nickel wall created a magnetic field gradient in the microchannel, and applied a magnetic translational force to the RBC. The motion of the RBC and the height position at which the RBC floated due to the balance of the magnetic force and the gravity was measured. Taking the magnetic field generated in the microchannel into account, the magnetic bulk susceptibility was obtained by the measured height position. The value was  $\chi = -0.161 \times 10^{-7}$  and agreed well with the values referring to other works.

**Keywords:** *Red blood cell, Magnetic field, Microchannel, Susceptibility*

### 1. INTRODUCTION

There are two major dynamic influences of the magnetic field on the red blood cell (RBC) motion considering the magnetic field distribution in which the RBC is placed. One is the magnetic rotary torque that is generated if the RBC is placed in a uniform magnetic field. This torque makes the RBC rotate so that the disc plane of the RBC is directed to the magnetic field (so call "RBC orientation"). The other one is the translational force that appears when the RBC is placed in the magnetic field with a gradient. The former force works mainly on the protein that composes the RBC membrane, and the latter one is attributed to the membrane and the presence of the hemoglobin in the RBC. Since the RBCs occupy a large amount of volume in the blood (40%) [1], these influences of the magnetic field on the RBC can affect the RBC behaviour and the blood flow characteristics: e.g. aggregation, thrombus and change in the fluid viscosity. On the other hand, recently, such magnetic forces are also used in micro-devices in order to manipulate individual RBCs for the purpose of sorting specific cells from other ones [2]. Therefore, it is important to understand the behaviour of the RBCs placed in a magnetic field from the viewpoints of fluid dynamics, medical science and micro-device technology.

Numerical simulation is a powerful tool to understand the blood flow characteristics on human vein and behaviour of RBCs in blood flows, or to design the micro-devices that handles biological flows. Various researches on modeling blood flows have been carried out in the past few decades [3]. Generally, these

models can be divided into two types of method: one is the bulk flow computation considering the RBC effects as the change in fluid properties and the other is the computation solving the motion of each single RBC. However, there are few models considering the influences of the magnetic field on the RBCs or the blood flow. Indeed, there are several models that can solve the magnetic field effect on particle motions suspended in fluids [5]. It is obvious, however, that such model cannot be applied to RBCs due to the difference in the shape and structure between a rigid spherical particle and a concave cell filled with cytoplasm.

In order to develop such numerical model, and to understand the magnetic characteristics of the RBC in fluid, it is necessary to measure the diamagnetic susceptibility and bulk susceptibility of the RBC. Yamagishi et al. [6] and Ueno & Suda [7] measured the diamagnetic susceptibility of the RBC measuring the intensity of the transmitted light. Takayasu et al. [8] measured the bulk susceptibility using magnetophoresis method. These methods, however, measure the bulk mean value of the RBC suspended fluid, or consider the RBC as spherical particles. The accuracy of the measurement, thus, may not be high enough to be applied to the numerical simulation.

In the present study, measurement of the single RBC motion in the suspended fluid was carried out using the microchannel and high-speed camera to measure the magnetic properties of the RBC. Using the microchannel has the advantage of easy flow control, small sample fluid requirement, and precise measurement of a single RBC. In the authors' previous paper [9], the relationship between the RBC rotational motion and time is measured from the video images, and is compared with numerical results in order to calculate the diamagnetic susceptibility. In the present paper, a microchannel with a wall made of nickel (a ferromagnetic material) is fabricated using electro-plating method. We will use this channel and measure the bulk susceptibility by measuring the height position of which the RBC levitates with the balance between the gravity force and magnetic translational force. The RBC height position is compared with the numerical results to calculate the diamagnetic susceptibility.

## 2. EXPERIMENTAL SETUP

### 2.1 Experimental Apparatus

The magnetic field generator (JASTEC Inc.; JMTD-10T100KDK) used in this study has a test bore of 100mm diameter surrounded by the super-conduction magnet coil. As the current is supplied to the coil, a uniform magnetic field is generated in the bore. Figure 4 shows the schematic view of the experimental apparatus. The optical system consists of a high-speed digital video camera (Vision Research; Phantom V7.3), optical pathway with a  $\times 20$  magnification objective lens (Olympus Co.; LMPLFLN20X) attached to the end, and a traversable stage. In order to reduce the influence of oscillation caused by the coolant system of the magnetic field generator, equipment is set up on the frame structure separately mounted on the ground. A stage on which the microchannel is attached is placed below the objective lens. In order to measure the height position of the RBC in the channel, namely the distance from the channel bottom wall, it is necessary to measure the motion of the RBC from the channel sidewall. Therefore, a mirror is installed in the pathway and flow is measured as shown in Fig. 1. The microchannel is illuminated by the LED lights from the bottom wall side of the channel. The distance between the stage and the high-speed camera located above the magnetic field generator is 1.5m. The recording rate and exposure time are 10fps and 1.5ms, respectively. The CCD resolution is  $800 \times 600$  pixels, and the spatial resolution of the video images is  $0.46 \mu\text{m}/\text{pixel}$ .

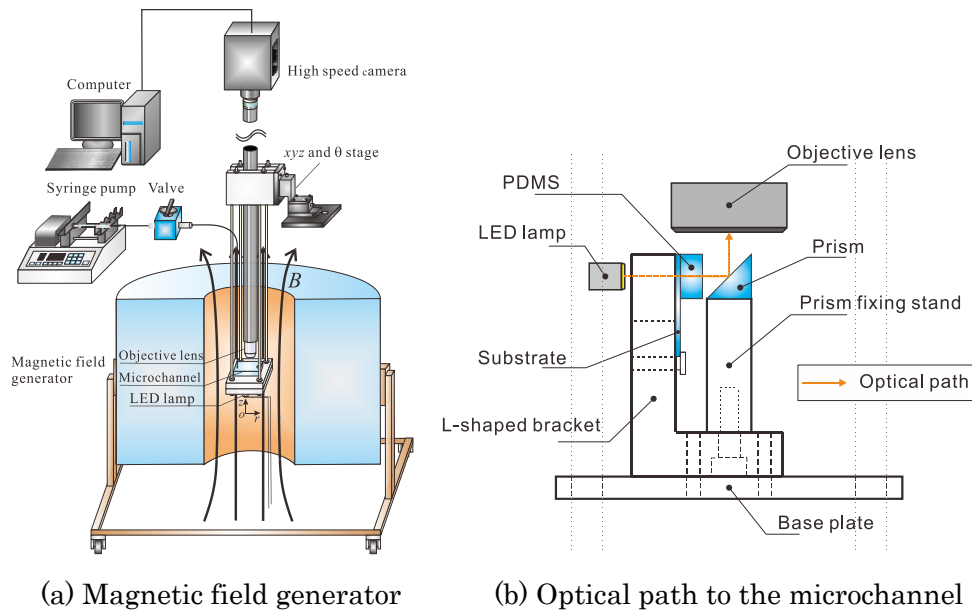


Figure 1: Experimental apparatus.

## 2.2 Microchannel

Figure 2 shows the schematic view of the microchannel and its coordinate system. The microchannel is made of PDMS (Shin-Etsu Chemical Co.; K-106) fabricated by a soft lithography process using SU-8 (Microchem Co.). The channel unit made of PDMS is attached to a slide glass by plasma bonding. The microchannel consists of three parts: the straight channel (test section), the inlet and outlet reservoirs. In order to create a magnetic field gradient in the microchannel, ferromagnetic body is needed to be inserted in the channel because only a uniform magnetic field can be generated in the bore by the equipment. Therefore, an straight nickel wall with width  $\times$  height  $\times$  length of  $50\mu\text{m} \times 50\mu\text{m} \times 5\text{mm}$  was first fabricated on the glass substrate applying the Nickel electroplating process using Omnicoat and SU-8 as the resist. The PDMS was then placed on the glass substrate as previously mentioned. Since the microchannel was placed perpendicularly to the magnetic field as shown in Fig. 1, the nickel wall becomes the channel bottom.

The test section has a rectangular cross-section with  $50\mu\text{m}$  in height and  $500\mu\text{m}$  in width. A droplet of the sample RBC suspension is placed on the inlet reservoir and the outlet reservoir is connected to a syringe pump with teflon tubes to aspirate the droplet of sample solution through the inlet and drive the solution in the microchannel. This aspiration method has an advantage that the amount of the sample fluid is much smaller than the method which pumps out the sample fluid from the syringe because only a droplet of the sample is needed to be placed at the inlet of the microchannel. Further, the time required for the sample to reach the test section was reduced markedly allowing the sedimentation problem of the RBC occurring in the tube and syringe to be avoided.

## 2.3 Preparation of RBC Suspended in Buffer Solution

A small amount of blood was taken from a healthy human donor. The blood was collected in a plastic tube filled with 1mL solution of phosphate buffered saline (PBS, Amresco Inc.; E404) to which 0.019mM ATP (adenosine 5-triphosphate, disodium salt, Oriental Yeast Co. Ltd.) was added. This blood suspension was centrifuged at 1000G for 5 minutes and then its supernatant was removed, and 1mL solution of PBS was added. This washing procedure was carried out twice and 1mL RBC suspension was obtained. Note that all experiments were performed within several minutes from the time when the RBC suspension was prepared.

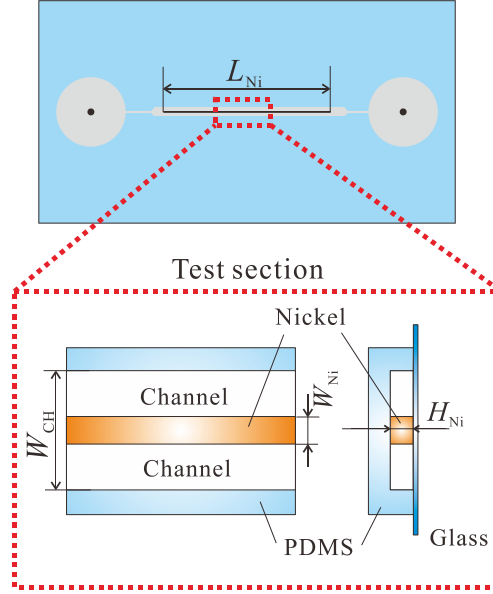


Figure 2: Schematic diagram of the microchannel with nickel wall.

## 2.4 Measurement Physics

To measure the diamagnetic susceptibility in steady state condition, the balance between the gravity and magnetic translational force is used in this study. Namely, if a magnetic field with a gradient in the height direction can be generated, the RBC should float at the position which these forces balance. The translational magnetic force  $F$  can be written as:

$$F = \frac{\partial}{\partial z} |B|^2 \frac{V_{RBC}}{2\mu_0} \chi \quad (1)$$

$\mu_0$  is the magnetic permeability in vacuum,  $V_{RBC}$  and  $\chi$  are the volume and diamagnetic susceptibility of the RBC. When the balance between the gravity force and the above magnetic force is considered, then  $\chi$  can be derived from the Eq. (2).

$$\chi = \frac{2\mu_0}{\frac{\partial}{\partial z} |B|^2} g (\rho_{RBC} - \rho_{fluid}) \quad (2)$$

$\rho_{RBC}$  and  $\rho_{fluid}$  are the density of the RBC and fluid, respectively.  $g$  is the acceleration of gravity.

## 2.5 Experimental Procedure and Conditions

In order to measure the RBC height position in steady state condition, the RBCs motion in microchannel with magnetic field gradient should be made under stationary fluid condition. The magnetic field generator can generate a highly precise uniform magnetic field, however the generator cannot activate the magnetic field immediately. Giving some dispersion to the RBC distribution in the microchannel and producing a stationary fluid condition is also difficult in the experiment. To overcome these problems, the following procedure is employed in the present experiment. The microchannel is placed in the bore where a steady magnetic field is formed. The RBC suspension is then aspirated by the syringe pump and supplied to the microchannel. In this state, the RBCs are dispersed in the channel due to the initial position and flow shear stress. After a steady flow is obtained, the valve installed between the microchannel and the syringe pump is closed to stop the flow instantaneously. This produces a stationary fluid condition in the channel. Note that the time required for the flow to stop is negligibly short compared with the time span of the RBC motion attributed to the magnetic field. The RBC is recorded by the high-speed camera until the translational motion of the RBC is completed. The flow rate before the valve is closed is  $10\mu\text{L}/\text{min}$  that results in the

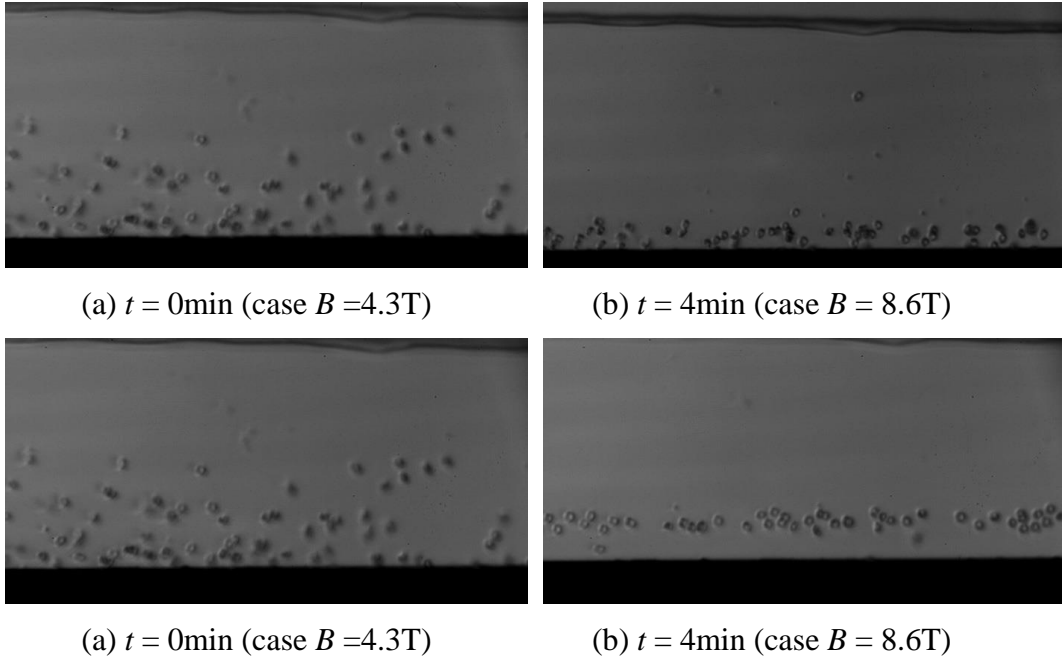


Figure 3: Snapshots of deoxygenated red blood cells suspended in fluids located above the channel bottom wall (nickel electroplated wall) measured by the high speed camera (The black area in the figure is the channel bottom wall).

cross-sectional mean velocity of 3.3mm/s. The measurements are carried out in the cases for magnetic field intensity of 4.3T and 8.6T, same as the conditions of the numerical simulation.

### 3. RESULTS AND DISCUSSION

#### 3.1 Measurement of Red Blood Cell Position

Figure 3 shows the snapshots of the RBC distribution recorded by the high speed camera in the cases of  $B = 4.3$  and  $8.6\text{T}$  at the time period of  $t = 0$  and  $4\text{min}$ . The RBC receives both the gravitational and magnetic forces, and will move upward or downward depending on which force is more dominant. In the case of (a)  $t = 0$ , the RBC position are dispersed in the channel owing to the influence of the flow before stopping at  $t = 0$ . As the time proceeds, the RBC moves in the height direction and the height position of the RBC will converge to a certain position.

The relationship between the RBC height position,  $h$ , and time,  $t$ , is summarized in Fig. 4. The error bar shown in the graph is obtained by the uncertainly analysis based on the ASME standard. Comparing the distributions of 4.3 and 8.6T,  $h$  in 8.6T case takes nearly 2 times larger value compared with the values of 4.3T case. This is reasonable since the magnetic force working on the RBC is proportional to the magnetic field intensity as shown in Eq. (2).

One may notice that  $h$  in both cases slightly decreases as the time elapse. It should be noted that it took only approximately 4~5min for the dispersed RBC to move and converge to the certain height. Therefore, this decrease of  $h$  should be attributed to another reason. We believe that it is due to the change of the RBC condition, namely, the deoxygenation of the RBC. It is known that as the haemoglobin in the RBC is deoxygenated, the bulk susceptibility of the RBC increases (negatively decrease). This was also confirmed in the authors' other experiments in which the motion of the RBC highly deoxygenated by applying the glutaraldehyde treatment was measured. In this case, the bulk susceptibility increased and showed a positive value. Therefore, during the measurement shown in Fig. 4, the RBC is deoxygenated gradually as the time elapsed, and the RBC moves closer to the channel bottom wall as the magnetic force decreases.

In addition to this, in Fig. 3, one can see that nearly all RBC are oriented with the biconcave surface parallel to the channel height direction. This is believed to be due to the fact that the RBCs attaches to

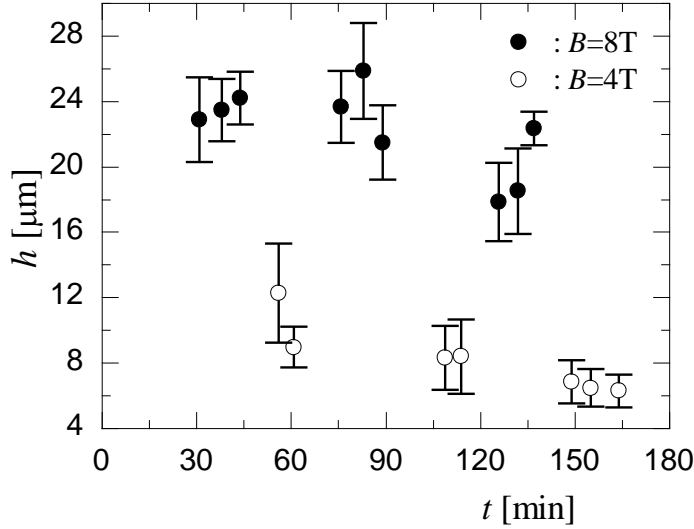


Figure 4: Time distribution of the distance between red blood cells and the channel bottom wall ( $t$  is the elapse time after the sample is prepared).

the channel sidewalls. As will be discussed in the next section, the RBC moves not only in the height direction but also spanwise direction since the gradient of the magnetic field is also formed in the that direction. The RBC, therefore, will reach and attach to the sidewalls as the time elapse. A question then arises if this phenomenon will affect the value  $h$ . Since the channel wall is treated by bovine serum albumin (SIGMA; A2153) in advance of the experiment, friction between the wall and the RBC is reduced markedly, and no adhesion effect was observed. The RBC still moved slowly but steadily in the height position after it attached to the sidewall. Therefore, after a sufficient elapse time,  $h$  should show a reliable value. Nevertheless, further discussion should be made on how significant this phenomenon will influence the uncertainty of the measurement.

### 3.2 Simulation of the Magnetic Field

To calculate the bulk susceptibility from the value  $h$  using Eq. (2), the intensity of the magnetic field gradient is required. In the present study, the magnetic field is obtained numerically. COMSOL Multiphysics (Ver. 4.3) was used to solve the Maxwell equation and calculate the three-dimensional magnetic field. Figure 5 shows the computational domain. The domain has a rectangular shape  $10 \times 250 \times 350 \mu\text{m}$ , and a rectangular area of  $10 \times 50 \times 50 \mu\text{m}$  made of nickel is attached to the channel as shown in the figure. Magnetic insulation condition are applied to the boundaries of the  $x$  and  $y$  directions. In the  $z$  direction, constant magnetic flux density  $B_z$  ( $=8.6\text{T}$  and  $4.3\text{T}$ ) are applied to the boundaries. In the Ni area, the magnetisation is considered to be saturated. And the saturation value  $I_z = 4.77 \times 10^5 \text{ A/m}$  is applied to the area. Other area is set to be non-magnetized.

Figure 6 shows the results of the magnetic field intensity,  $B$ , and its gradient,  $\partial B^2 / \partial y$  and  $\partial B^2 / \partial z$ , distributions in the case of  $B = 8.6\text{T}$ . The area of Ni material is indicated by the hatching. Since the magnetic field shows a symmetric distribution with the centreline of the channel, the area which corresponds to the experiment ( $y = 100 \sim 150 \mu\text{m}$ , and  $z = 200 \mu\text{m}$ ) is discussed here.

The RBC used in the experiment shows diamagnetism characteristic, and a force with opposite sign to the gradient of the magnetic field will appear. For  $\partial B^2 / \partial z$  in Fig. 6 (b), negative value is obtained therefore a magnetic force in the  $z$  positive direction will work on the RBC. Particularly near the Ni wall a very steep gradient, and hence a strong force is generated.

On the other hand, the distribution of the  $y$  direction components shows that in the area of  $100 < y < 125 \mu\text{m}$ , a positive gradient in the  $y$  direction appears which produces a force in the negative direction. In the area of  $125 < y < 150 \mu\text{m}$ , a symmetric tendency is observed. Due to these forces, therefore, the

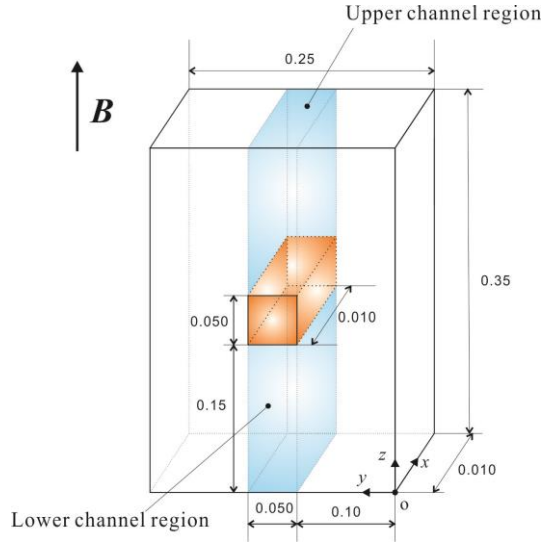
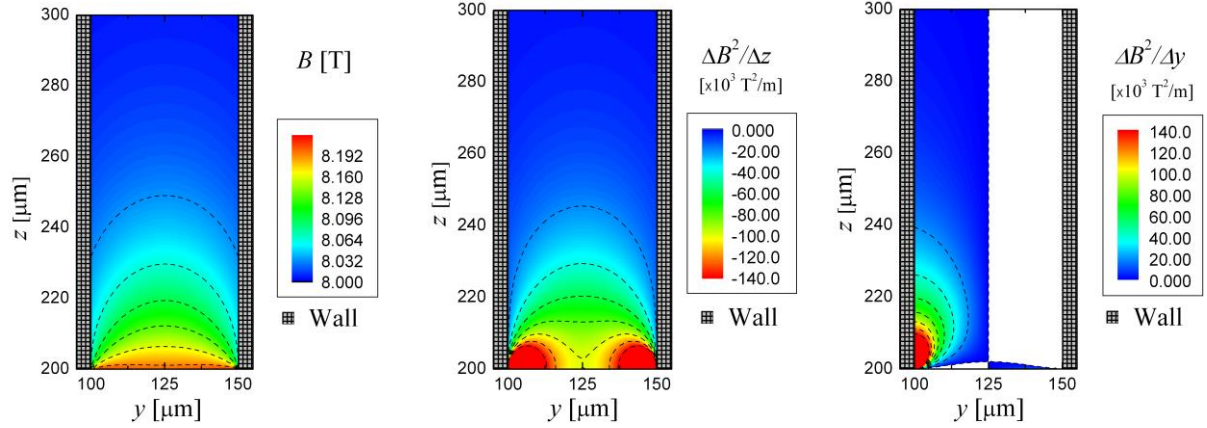


Figure 5: Computational domain (the unit is  $\mu\text{m}$ ).



(a) Magnetic field intensity (b) Magnetic field gradient  $z$  (c) Magnetic field gradient  $y$

Figure 6: Magnetic field distributions

RBCs will head toward the channel sidewalls. This agrees qualitatively with the experimental results shown in the previous section.

From the magnetic field distribution and the predicted trajectory of the RBC, depending on its initial position, most of the RBC will contact the channel sidewall before it reaches the specific point where the forces balance. However, as discussed above, the RBC is believed to not adhere with the wall, and will move along it in the height direction until it reaches the force-balancing height. From this reason, we will first measure the height position,  $h$ , from the experiment and then calculate the magnetic field gradient at that position of the channel sidewall. The bulk susceptibility is then obtained from Eq. (2).

### 3.3 Measurement of the Susceptibility

Following the procedure shown in Sections 2.4 and 3.2, the bulk susceptibility  $\chi$  is calculated in this section. It should be noted that the susceptibility obtained from the sequence is the difference between the susceptibility of the RBC and the solution ( $\chi = \chi_{\text{RBC}} - \chi_{\text{fluid}}$ ). Generally, RBCs are suspended in fluid, a solution of which the magnetic properties are similar to PBS. Therefore, as shown in other papers,  $\chi$  is the value which becomes practically important and will be used in the present paper for measurement.

Figure 7 shows the relationship between,  $\chi$ , and the elapse time,  $t$ , in the cases of 4.3 and 8.6T. In both cases,  $\chi$  decreases as the time elapse. This is because oxygen was released from the hemoglobin with time and the RBC was deoxidized as discussed in the previous section. Comparing the values of 4.3

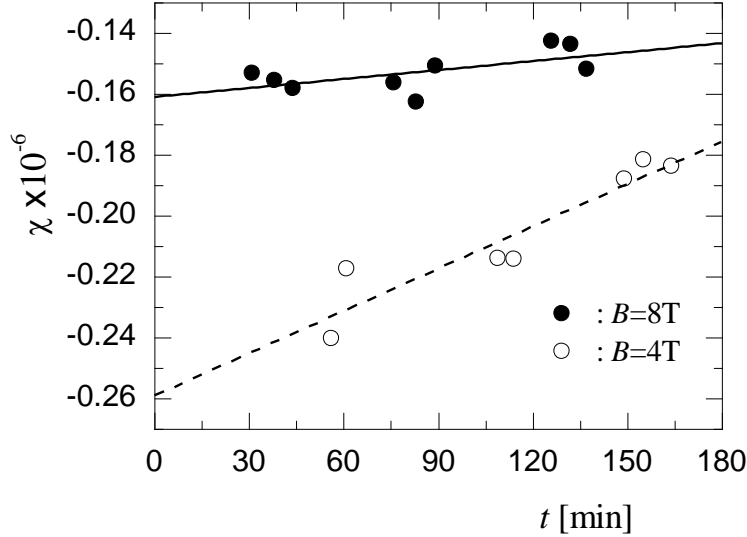


Figure 7: Time distribution of the distance between red blood cells and the channel bottom wall ( $t$  is the elapse time after the sample is prepared).

and 8.6T cases, we can see that although the samples with same condition were used during the experiment, the value  $\chi$  and its decrease ratio differs largely.

The bulk susceptibility we would like to obtain is the value of those which are not deoxygenated and is normal. Therefore,  $\chi$  at the time  $t=0$  was obtained by using the least mean square approximation. The value was  $\chi = -0.161 \times 10^{-7}$  in the case of 8.6T. This value corresponded agreed well with  $\chi = -0.185 \times 10^{-7}$ , which is the value measured by Zborowski et al. [9] using the method considering the balance between the forces of the flow and magnetic field. The reason for the discrepancy can be twofold. The first one is the intensity of the magnetic field gradient. As shown in Fig. 6, a very sharp gradient is generated near the nickel wall. As the position of the RBC gets closer to the wall, the magnetic force measured becomes more sensitive to the height position of the RBC. The measurement accuracy, therefore, decreases in this case. The second one is due to the fact that the magnetic force in the spanwise direction increases as the RBC height decreases. In this case, a strong force which pushes the RBC to the wall is generated. Although the RBC will move in the height direction after contacting the channel sidewall, a larger normal force, namely a larger wall friction, can incur an increase of the uncertainty in the height position at which the RBC converges.

#### 4. CONCLUSION

Measurement of the bulk susceptibility  $\chi$  of the red blood cell (RBC) was carried out using a high intensity magnetic field generator, microchannel and high speed camera. A nickel plating process was applied to fabricate a ferromagnetic channel wall. The height position at which the RBC levitated due to the balance between the gravity and magnetic force was measured. Numerical simulation was carried out to calculate the magnetic field in the microchannel. The magnetic field gradient at the position at the RBC position was thus obtained to calculate  $\chi$ . The measured  $\chi$  was  $-0.161 \times 10^{-7}$  that agreed reasonably well with the one in other references confirming the of the present method.

#### ACKNOWLEDGEMENT

This work was financially supported by the Ministry of Education, Culture, Sports and Science and Technology of Japan.

#### REFERENCES

- [1] M. Sugawara, and N. Maeda, *Hemorheology and Blood Flow*, CORONA Publishing, Japan, 2003.



- [2] B. Y. Qu, Z. Y. Wu, F. Fang, Z. M. Bai, D. Z. Yang, and S. K. Xu, A glass microfluidic chip for continuous blood cell sorting by a magnetic gradient without, *Analytical and bioanalytical chemistry*, **392**, pp.1317-1324, 2008.
- [3] L. Grinberg, E. Cheever, T. Anor, J. R. Madsen, and G.E.Karniadakis, Modeling Blood Flow Circulation in Intracranial Arterial Networks: A Comparative 3D/1D Simulation Study, *Annals of Biomedical Engineering*, **29**, pp.297-309, 2011.
- [4] J. W. Haverkort, S. Kenjeres, and C. R. Kleijn, Computational Simulations of Magnetic Particle Capture in Arterial Flows, *Annals of Biomedical Engineering*, **37**, pp.2436-2448, 2009.
- [5] A. Yamagashi, T. Takeuchi, T. Hagashi, and M. Date, Diamagnetic Orientation of Blood Cells in High Magnetic Field, *Physica B: Physics of Condensed Matter*, **177**, pp.523-526, 1992.
- [6] S. Ueno and T. Suda, Magnetic Orientation of Red Blood Cell Membranes, *IEEE Transactions on Magnetics*, **30**, pp.4713-4715, 1994.
- [7] M. Takayasu, D.R. Kelland, and J.V. Minervini, Continuous Magnetic Separation of Blood Components from Whole Blood, *IEEE Transactions on Applied Superconductivity*, **10**, pp.927-930, 2000.
- [8] K. Tatsumi, Y. Komori, T. Arakawa, K. Nishitani and K. Nakabe, Development of a Numerical Model for Single Red Blood Cell Motions in Stationary Fluid in the Presence of Uniform Magnetic Field, *Progress in Computational Fluid Dynamics*, **13**, pp. 228-241, 2013.
- [9] M. Zborowski, G.R. Ostera, L.R. Moore, S. Milliron, J.J. Chalmers, A.N. Schechter, Red Blood Cell Magnetophoresis, *Biophysical Journal*, **84**, pp. 2638-2645, 2003.
- [10] S. Chikasumi, *Physics of Ferromagnetic Body*, Shokabo, 2008.